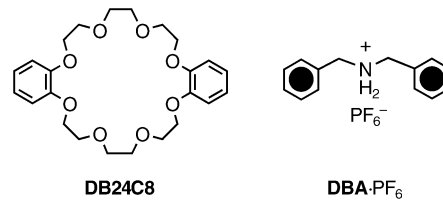


Magic Ring Rotaxanes by Olefin Metathesis**

Andreas F. M. Kilbinger, Stuart J. Cantrill,
Andrew W. Waltman, Michael W. Day, and
Robert H. Grubbs*

Rotaxanes^[1] are mechanically interlocked molecules composed of a dumbbell-shaped component around which one or more macrocycles are trapped. In some cases, the ability to move—in a controlled fashion—these intimate noncovalently linked components with respect to one another, has led to the creation of molecular switches^[2] which have had a significant impact on the emerging field of molecular computing.^[3] Although the majority of rotaxane syntheses to date have relied upon kinetic control,^[4] that is, employing an irreversible final reaction step, a resurgence in the popularity of dynamic covalent chemistry^[5] has spurred an interest in pursuing rotaxane formation under thermodynamic control.^[6] Reversible reactions^[7] utilized for this purpose include the formation (and subsequent associated cleavage) of functional groups such as imines^[8] and disulfides.^[9] Olefin metathesis, mediated by functional-group-tolerant ruthenium alkylidene catalysts,^[10] has been used in the thermodynamically controlled synthesis of a [2]catenane,^[8d,11] and, more recently, has been applied^[12] to the anion-templated synthesis of a [2]rotaxane. One of the most established^[13] supramolecular synthons employed in the construction of rotaxanes exploits the mutual recognition exhibited by secondary dialkylammonium ($R_2NH_2^+$) ions and suitably sized crown ethers,^[14] most notably dibenzo[24]crown-8 (**DB24C8**). Here, we combine



DB24C8 **DBA-PF₆-**

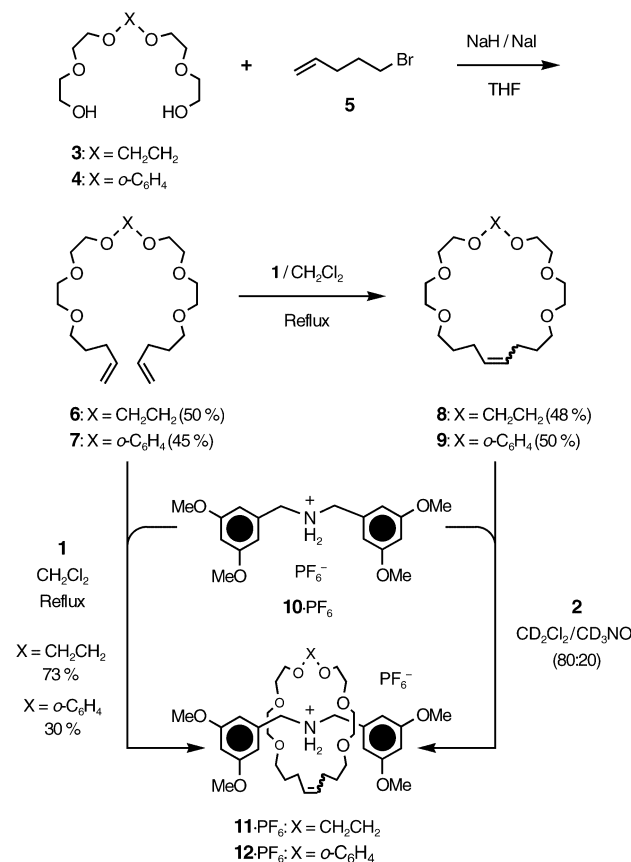
[*] Prof. R. H. Grubbs, Dr. A. F. M. Kilbinger, Dr. S. J. Cantrill, A. W. Waltman
Arnold and Mabel Beckman Laboratory of Chemical Synthesis
Division of Chemistry and Chemical Engineering
Pasadena, CA 91125 (USA)
Fax: (+1) 626-564-9297
E-mail: rhg@caltech.edu
Dr. M. W. Day
Beckman Institute
X-Ray Crystallography Laboratory
California Institute of Technology
Pasadena, CA 91125 (USA)

[**] A.F.M.K. thanks the Alexander von Humboldt Foundation for a Feodor-Lynen Research Fellowship. We thank Dr. Mona Shahgholi for performing the mass spectrometric analyses, Dr. Jennifer Love for assisting with initial NMR spectroscopic measurements, and Dr. Steven Goldberg for valuable comments regarding this manuscript.

 Supporting information for this article is available on the WWW under <http://www.angewandte.org> or from the author.

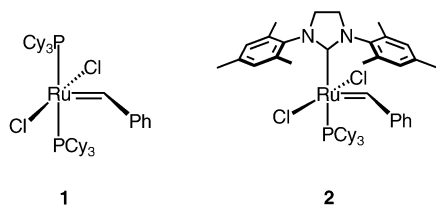
the reliability of this supramolecular synthon with the versatile reversible ring-closing-metathesis (RCM) reaction to form rotaxanes under thermodynamic control.

In an effort to mimic the significant $R_2NH_2^+$ ion binding capability of **DB24C8**, our first target macrocycle was designed such that it retained many of the desirable features of the original crown ether. Pentaethylene glycol (**3**) was bisalkylated with 5-bromo-1-pentene (**5**) to afford (Scheme 1)



Scheme 1. Synthesis of the olefin macrocycles **8** and **9**, via their corresponding diolefin precursors **6** and **7**, respectively. Rotaxane synthesis can be achieved through either a ring-closing-metathesis approach, by utilizing **6** and **7** as starting materials (lower left pathway), or by a magic ring synthesis in which the preformed macrocycles **8** and **9** are employed (lower right pathway).

the terminal diolefin **6** in moderate yield. Treatment of **6** with $(PCy_3)_2(Cl)_2Ru=CHPh$ (**1**)^[15] under dilute conditions, gave the 24-membered olefinic crown ether analogue **8** as a mixture of *E* and *Z* isomers. The constitution of **8** is strikingly similar in nature to the macrocyclic skeleton of **DB24C8**, thereby satisfying our primary design criterion outlined



above. Indeed, subsequent ¹H NMR spectroscopic investigations revealed that **8** does interact with dibenzylammonium hexafluorophosphate (**DBA·PF₆**) to form a 1:1 complex with a threaded geometry, that is, a pseudorotaxane. The association constant (K_a)^[16] for this process is 100 M^{-1} (CD_3CN , 295 K), which is slightly lower than the value of 320 M^{-1} reported^[17] for **DB24C8** under similar conditions. The major contributing factor^[18] to this reduced binding affinity arises presumably from the “loss” of two ether oxygen atoms—on going from **DB24C8** to **8**—thereby decreasing the hydrogen-bonding potential between the two components.

Encouraged by these findings, the RCM reaction of the terminal diolefin **6** was repeated (Scheme 1) in the presence of a dumbbell-shaped template containing an ammonium ion, namely bis(3,5-dimethoxybenzyl)ammonium hexafluorophosphate (**10·PF₆**)^[19] to afford, in 73 % yield, the corresponding [2]rotaxane **11·PF₆** as a mixture of *E* and *Z* isomers. The significant templating effect of the $R_2NH_2^+$ ion can be appreciated by comparing this reaction with the untemplated macrocyclization of **6** to form **8**. Whereas the untemplated reaction is carried out at about 5 mM (to avoid oligo/polymerization) and yields only 48 % of the desired macrocycle, the templated reaction can be performed at much higher concentrations (ca. 100 mM in this case) to give 73 % of the ring-closed product, namely the rotaxane. Subsequent characterization by ¹H and ¹³C NMR spectroscopy, mass spectrometry (electrospray), and single-crystal X-ray analysis^[20] (Figure 1)

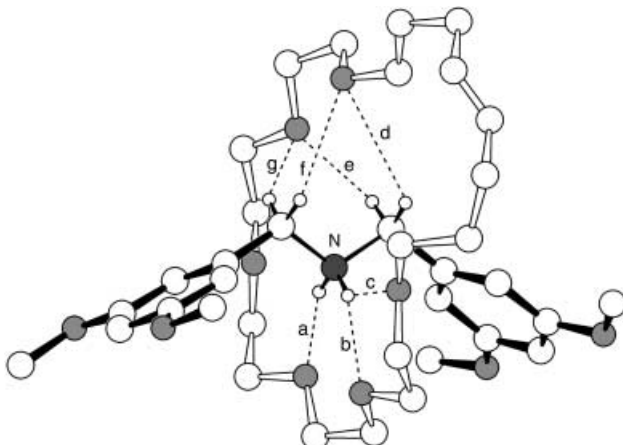


Figure 1. Ball-and-stick representation of the solid-state structure of the [2]rotaxane **11·PF₆**. Hydrogen-bonding geometries [$N^+...O$, $[H...O]$ Å, $[N^+H...O]$ °]: a) 2.86, 2.04, 156; b) 2.87, 2.08, 142; c) 3.03, 2.27, 137; [C...O], $[H...O]$ Å, $[C-H...O]$ °: d) 3.35, 2.89, 109; e) 3.41, 2.48, 161; f) 3.34, 2.88, 110; g) 3.53, 2.66, 152.

confirmed unambiguously the interlocked nature of **11·PF₆**. The cluster of peaks in the carbon–carbon double bond region of the final difference map, as well as displacement ellipsoids, some anomalous bond lengths, and the high *R* and GOF values indicate a degree of conformational disorder of this hydrocarbon loop and suggest that a mixture of *E* and *Z* isomers are present. No attempt was made to model this disorder. Subsequent hydrogenation ($H_2/Pd/C$) of **11·PF₆** gave the saturated rotaxane **13·PF₆** (see Supporting Information),

in which the two olefin isomers collapsed into a single species, thereby facilitating the spectroscopic analysis.

Derivatization of the crown ether, to allow for the construction of extended supramolecular arrays,^[21] is most easily achieved through a benzo ring that is fused to the parent macrocycle. The benzo analogues of both **6** and **8** were prepared (Scheme 1) in a similar fashion. Alkylation of the known^[22] diol **4** afforded the diolefin **7**, which was subsequently converted into the desired benzocrown ether analogue **9** through a RCM reaction mediated by **1**. The K_a value for the interaction between **9** and **DBA**·PF₆ was shown^[23] to be about 10 M⁻¹ (CD₃CN, 295 K), approximately one order of magnitude lower than that observed for **8**. This decreased affinity for ammonium ion binding can be attributed to the reduced hydrogen-bonding ability of the benzo-substituted macrocycle, namely, two of the oxygen atom donors are now phenolic in nature and are consequently less basic. Nonetheless, the benzo-substituted rotaxane **12**·PF₆ (*E/Z* mixture) was obtained (Scheme 1) upon the RCM reaction of **7** in the presence of **10**·PF₆, albeit in a reduced yield (30% instead of 73%). In addition to NMR spectroscopic and mass spectrometric characterization, X-ray quality single crystals^[24] of this compound (Figure 2) were obtained upon slow evaporation of an EtOAc solution. The crystal structure of **12**·PF₆ contains both *E* and *Z* isomers, which are present at the same site in an approximately 1:1 ratio. Reasonable geometries in this disordered region were only obtained with a number of restraints. Once again, the *E/Z* mixture contributes to the high *R* and GOF values obtained.

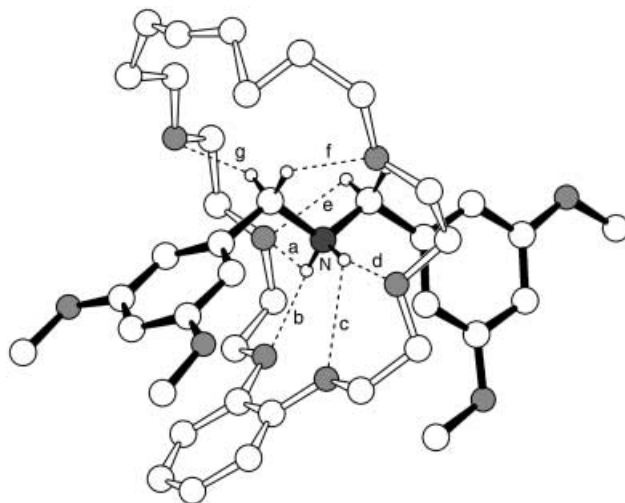


Figure 2. Ball-and-stick representation of the solid-state structure of the benzo-substituted [2]rotaxane **12**·PF₆. Hydrogen-bonding geometries [N⁺...O], [H...O] Å, [N⁺—H...O] °: a) 3.10, 2.55, 119; b) 3.03, 2.14, 162; c) 3.08, 2.55, 117; d) 2.88, 1.98, 167; [C...O], [H...O] Å, [C—H...O] °: e) 3.14, 2.53, 120; f) 3.41, 2.56, 143; g) 3.48, 2.53, 161.

To demonstrate the inherent reversibility of rotaxane formation by olefin metathesis, a “magic ring”^[11a] experiment was performed in which the rotaxane was assembled (Scheme 1) directly from its preformed components, namely, the dumbbell and the macrocycle. A CD₂Cl₂/CD₃NO₂ (80:20)

solution^[25] containing equimolar quantities of crown ether **8** and the dumbbell-shaped compound **10**·PF₆ was prepared. Prior to the addition of any catalyst, ¹H NMR spectroscopic analysis revealed that, as expected, the terminally bulky-substituted secondary ammonium cation **10**⁺ cannot pass through the cavity of the 24-membered macrocyclic ring. Enabling the metathesis pathway, however, upon the addition of (IMesH₂)(PCy₃)(Cl)₂Ru=CHPh (**2**)^[26] (10 mol %), allows the system to equilibrate to a thermodynamic minimum (a process driven by the creation of N⁺—H...O and C—H...O hydrogen bonds), and results in the formation of the [2]rotaxane **11**·PF₆. This transformation was monitored (Figure 3) by ¹H NMR spectroscopy, and equilibrium

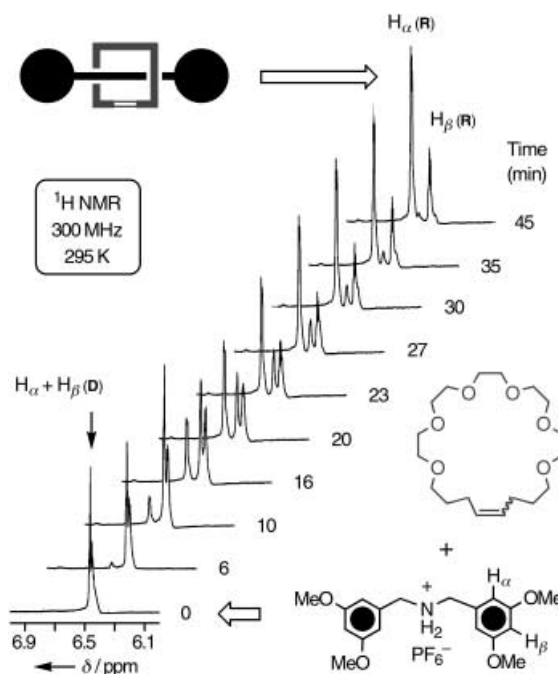


Figure 3. Partial ¹H NMR spectra showing the change over time in the environment of H_α and H_β as the dumbbell (D) component converts into the rotaxane (R) during the magic ring synthesis in which macrocycle **8** and **10**·PF₆ were employed as starting materials.

(>95% interlocked species) was achieved in 45 minutes. Spectral assignments were made by comparison to an authentic sample of the rotaxane isolated previously in the RCM approach, and mass spectrometric analysis also confirmed that the major component in solution was, indeed, the [2]rotaxane **11**·PF₆.

In an analogous fashion, the magic ring experiment was repeated with the benzo-derivative **9** and resulted (Figure 4) in a similar outcome. In this case, the equilibrium position is reached in less time (ca. 20 min), and affords a smaller proportion of the interlocked species (ca. 85% of the [2]rotaxane **12**·PF₆), which presumably reflects the reduced affinity of this particular macrocycle for secondary dibenzyl-ammonium ions. No decrease of catalyst activity was observed over the duration of the magic ring syntheses described above, as indicated by the undiminished intensity of the carbene (benzylidene) singlet of the catalytic species (δ =

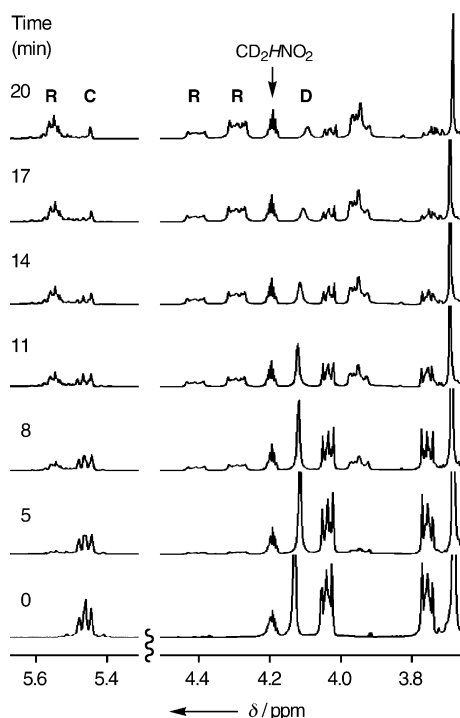


Figure 4. Partial ^1H NMR spectra showing the change over time during the magic ring synthesis in which macrocycle **9** and **10**- PF_6^- were employed as starting materials. The singlet at $\delta = 4.15$ ppm, which arises from the methylene proton of the free dumbbell (**D**) component, diminishes over time. Conversely, the characteristic multiplets centered around $\delta = 4.27$ and 4.40 ppm indicate the formation of two new interlocked products, namely, the *E* and *Z* isomers, respectively, of the corresponding [2]rotaxane **12**- PF_6^- (**R**). Furthermore, the multiplet at $\delta = 5.45$ ppm, corresponding to the olefinic protons of the free crown ether analogue (**C**), also reduces in intensity at the expense of the multiplet just downfield from it—which corresponds to the olefinic resonances of the (*E/Z*) rotaxane mixture (**R**).

19.0 ppm) in the ^1H NMR spectrum. Furthermore, the magic ring syntheses of the [2]rotaxanes employ the more active metathesis catalyst **2**, and, under this particular set of conditions, the transformations occur with very high yields that approach, in the case of the non-benzo system, quantitative numbers.

In conclusion, diolefin macrocyclic precursors have been shown to cyclize around an appropriately substituted dibenzylammonium salt to produce the corresponding [2]rotaxanes. Exploiting ruthenium carbene mediated olefin metathesis in this “clipping” procedure allows for the assembly process to occur in a reversible fashion, namely, it can operate under thermodynamic control. This dynamic feature can be utilized to synthesize mechanically interlocked molecules under magic ring conditions, whereby preformed components can be exposed to the necessary catalytic agent (**1** or **2** in this case) causing the macrocycle to open and close repeatedly while the system strives to reach a thermodynamic minimum. The successful application of this methodology to the synthesis of simple [2]rotaxanes, has enabled the creation of other, more intricate, interlocked molecular architectures (for example, catenanes,^[1] daisy chains,^[21] and other interlocked polymeric systems) to be explored. Moreover, the ability to drive these

systems to almost quantitative conversion allows for the pursuit of high-molecular-weight polymers with novel interlocked architectures.

Experimental Section

General procedure for “magic ring” experiments: Catalyst **2** (0.8 mg, 10^{-3} mmol) was added under a dry N_2 atmosphere to a solution of unsaturated crown ether **8** or **9** (10 mmol) and **10**- PF_6^- (4.6 mg, 10^{-2} mmol) in $\text{CD}_2\text{Cl}_2/\text{CD}_3\text{NO}_2$ (80:20, 1.0 mL). The reaction was followed by ^1H NMR spectroscopy under ambient conditions. For all other experimental procedures and characterization data, see the Supporting Information.

Received: February 13, 2003 [Z51167]

Published online: July 3, 2003

Keywords: macrocycles · metathesis · rotaxanes · ruthenium · template synthesis

- [1] a) D. B. Amabilino, J. F. Stoddart, *Chem. Rev.* **1995**, *95*, 2725–2828; b) *Molecular Catenanes, Rotaxanes and Knots* (Eds.: J.-P. Sauvage, C. Dietrich-Buchecker), Wiley-VCH, Weinheim, **1999**.
- [2] a) V. Bermudez, N. Capron, T. Gase, F. G. Gatti, F. Kajzar, D. A. Leigh, F. Zerbetto, S. W. Zhang, *Nature* **2000**, *406*, 608–611; b) J.-P. Collin, C. Dietrich-Buchecker, P. Gaviña, M. C. Jimenez-Molero, J.-P. Sauvage, *Acc. Chem. Res.* **2001**, *34*, 477–487.
- [3] a) A. R. Pease, J. F. Stoddart, *Struct. Bonding (Berlin)* **2001**, *99*, 189–236; b) Y. Luo, C. P. Collier, J. O. Jeppesen, K. A. Nielsen, E. Delonno, G. Ho, J. Perkins, H.-R. Tseng, T. Yamamoto, J. F. Stoddart, J. R. Heath, *ChemPhysChem* **2002**, *3*, 519–525.
- [4] For recent examples of kinetically controlled rotaxane syntheses, see a) J. E. H. Binston, F. Marken, H. L. Anderson, *Chem. Commun.* **2001**, 1046–1047; b) S.-H. Chiu, S. J. Rowan, S. J. Cantrill, J. F. Stoddart, A. J. P. White, D. J. Williams, *Chem. Eur. J.* **2002**, *8*, 5170–5183.
- [5] a) J.-M. Lehn, *Chem. Eur. J.* **1999**, *5*, 2455–2463; b) S. J. Rowan, S. J. Cantrill, G. R. L. Cousins, J. K. M. Sanders, J. F. Stoddart, *Angew. Chem.* **2002**, *114*, 938–993; *Angew. Chem. Int. Ed.* **2002**, *41*, 898–952.
- [6] For the earliest reported examples of a rotaxane synthesis that utilizes reversible formation of a covalent bond, see I. T. Harrison, *J. Chem. Soc. Chem. Commun.* **1972**, 231–232.
- [7] Certain kinetically labile metal–ligand interactions have also been exploited, as the reversible “reaction” step, in the formation of dynamic (organometallic) rotaxanes; for a recent example, see C. A. Hunter, C. M. R. Low, M. J. Packer, S. E. Spey, J. G. Vinter, M. O. Vysotsky, C. Zonta, *Angew. Chem. Int. Ed.* **2001**, *113*, 2750–2754; *Angew. Chem. Int. Ed.* **2001**, *40*, 2678–2682.
- [8] a) S. J. Cantrill, S. J. Rowan, J. F. Stoddart, *Org. Lett.* **1999**, *1*, 1363–1366; b) P. T. Glink, A. I. Olivia, J. F. Stoddart, A. J. P. White, D. J. Williams, *Angew. Chem.* **2001**, *113*, 1922–1927; *Angew. Chem. Int. Ed.* **2001**, *40*, 1870–1875; c) D. A. Leigh, P. J. Lusby, S. J. Teat, A. J. Wilson, J. K. Y. Wong, *Angew. Chem. Int. Ed.* **2001**, *113*, 1586–1591; *Angew. Chem. Int. Ed.* **2001**, *40*, 1538–1543.
- [9] a) A. G. Kolchinski, N. W. Alcock, R. A. Roesner, D. H. Busch, *Chem. Commun.* **1998**, 1437–1438; b) T. Oku, Y. Furusho, T. Takata, *J. Polym. Sci.* **2003**, *41*, 119–123.
- [10] T. M. Trnka, R. H. Grubbs, *Acc. Chem. Res.* **2001**, *34*, 18–29.
- [11] a) T. J. Kidd, D. A. Leigh, A. J. Wilson, *J. Am. Chem. Soc.* **1999**, *121*, 1599–1600; for other catenane syntheses employing RCM, see b) D. G. Hamilton, N. Feeder, S. J. Teat, J. K. M. Sanders, *New J. Chem.* **1998**, 1019–1021; c) M. Weck, B. Mohr, J.-P.

Sauvage, R. H. Grubbs, *J. Org. Chem.* **1999**, *64*, 5463–5471, respectively.

[12] J. A. Wisner, P. D. Beer, M. G. B. Drew, M. R. Sambrook, *J. Am. Chem. Soc.* **2002**, *124*, 12469–12476. During the course of our investigations, this report of rotaxane formation, by using ring-closing-olefin metathesis, appeared in the literature. Although the authors note that the metathesis reaction is under thermodynamic control, this aspect of the reaction is not investigated further.

[13] a) A. G. Kolchinski, D. H. Busch, N. W. Alcock, *J. Chem. Soc. Chem. Commun.* **1995**, 1289–1291; b) S. J. Cantrill, A. R. Pease, J. F. Stoddart, *J. Chem. Soc. Dalton Trans.* **2000**, 3715–3734, and references therein.

[14] S. J. Cantrill, D. A. Fulton, A. M. Heiss, A. R. Pease, J. F. Stoddart, A. J. P. White, D. J. Williams, *Chem. Eur. J.* **2000**, *6*, 2274–2287.

[15] P. Schwab, R. H. Grubbs, J. W. Ziller, *J. Am. Chem. Soc.* **1996**, *118*, 100–110.

[16] The association constant for this slowly equilibrating system was determined using the single-point method, see J. C. Adrian, C. S. Wilcox, *J. Am. Chem. Soc.* **1991**, *113*, 678–680. It should be noted that, in this case, the K_a value reflects a total association constant, which combines the contributions from both the *cis* and *trans* isomers of the crown ether present in solution.

[17] P. R. Ashton, R. A. Bartsch, S. J. Cantrill, R. E. Hanes, Jr., S. K. Hickingbottom, J. N. Lowe, J. A. Preece, J. F. Stoddart, V. S. Talanov, Z.-H. Wang, *Tetrahedron Lett.* **1999**, *40*, 3661–3664.

[18] Hydrogenation of **8** affords the saturated crown ether **15**, which was shown (by ^1H NMR spectroscopy) to bind dibenzylammonium hexafluorophosphate with a K_a value of 90M^{-1} . This value differs only slightly from that observed for **8**, thus suggesting that the carbon–carbon double bond has little effect upon the ability to bind secondary ammonium ions.

[19] S. J. Cantrill, M. C. T. Fyfe, A. M. Heiss, J. F. Stoddart, A. J. P. White, D. J. Williams, *Org. Lett.* **2000**, *2*, 61–64.

[20] Crystal data for **11**·PF₆: [C₃₆H₅₈NO₁₀][PF₆]; $M_r = 809.80$; 0.19 \times 0.20 \times 0.24 mm; colorless; monoclinic; space group P2₁/n (no. 14), $Z = 4$; $a = 13.3814(7)$, $b = 19.3278(10)$, $c = 16.1791(8)$ Å, $\beta = 109.105(1)$ °; $V = 3594.0(4)$ Å³; $\rho_{\text{calcd}} = 1.360$ g cm⁻³; Mo_{Kα} radiation ($\lambda = 0.71073$ Å); $2\theta_{\text{max}} = 56.8$ °; ω -scans on a SMART 1000 ccd; $T = 98$ K; 67646 reflections measured (all 9326 unique used); $-17 \leq h \leq 17$, $-25 \leq k \leq 25$, $-21 \leq L \leq 20$; Lorentz factor but no absorption correction ($\mu = 0.15$ mm⁻¹) applied; structure solved and refined with full-matrix least-squares on F^2 with SHELXL-97^[27]; 9326 data, 0 restraints, and 583 parameters; $R(6046 \text{ reflections} > 2\sigma(I), \text{ all data}) = 0.070$, 0.107; $R_w(6046 \text{ reflections} > 2\sigma(I), \text{ all data}) = 0.109$, 0.113; $S = 2.62$; hydrogen atoms on the macrocycle were riding, while those on the cation were unrestrained; greatest final electron density difference excursions of 1.41 e·Å⁻³ at 1.02 Å from H(11A) and -1.36 e·Å⁻³ at 0.42 Å from C(12).^[28]

[21] S. J. Cantrill, G. J. Youn, J. F. Stoddart, D. J. Williams, *J. Org. Chem.* **2001**, *66*, 6857–6872.

[22] B. Colonna, L. Echegoyen, *Chem. Commun.* **2001**, 1104–1105.

[23] Hydrogenation of olefin macrocycle **9** affords the saturated analogue **16**, which shows little change in the binding affinity for **DBA**·PF₆ ($K_a \sim 10\text{M}^{-1}$).

[24] Crystal data for **12**·PF₆: [C₄₀H₅₈NO₁₀][PF₆]; $M_r = 857.84$; 0.24 \times 0.31 \times 0.33 mm; colorless; monoclinic; space group P2₁/n (no. 14), $Z = 4$; $a = 14.3407(6)$, $b = 19.2063(8)$, $c = 15.8720(7)$ Å, $\beta = 107.353(1)$ °; $V = 4172.7(3)$ Å³; $\rho_{\text{calcd}} = 1.366$ g cm⁻³; Mo_{Kα} radiation ($\lambda = 0.71073$ Å); $2\theta_{\text{max}} = 55.4$ °; ω -scans on a SMART 1000 ccd; $T = 98$ K; 83324 reflections measured (all 9644 unique used); $-18 \leq h \leq 18$, $-25 \leq k \leq 24$, $-21 \leq L \leq 21$; Lorentz factor but no absorption correction ($\mu = 0.15$ mm⁻¹) applied; structure solved and refined with full-matrix least-squares on F^2 with SHELXL-97^[27]; 9644 data, 235 restraints (distance, planarity, and anisotropic displacement parameter restraints in the macrocyclic double bond region which was disordered ca. 1:1 *E*:*Z*), and 582 parameters; $R(6838 \text{ reflections} > 2\sigma(I), \text{ all data}) = 0.063$, 0.090; $R_w(6838 \text{ reflections} > 2\sigma(I), \text{ all data}) = 0.105$, 0.107; $S = 3.48$; all hydrogen atoms were riding on attached atoms; greatest final electron density difference excursions of 0.78 e·Å⁻³ and -0.82 e·Å⁻³.^[28]

[25] CD₃NO₂ is required to ensure complete dissolution of **10**·PF₆.

[26] IMesH₂ = 1,3-dimesityl-4,5-dihydroimidazol-2-ylidene, see M. Scholl, S. Ding, C. W. Lee, R. H. Grubbs, *Org. Lett.* **1999**, *1*, 953–956.

[27] G. M. Sheldrick, SHELXL-97, Program for Structure Refinement, University of Göttingen, Göttingen (Germany), **1997**.

[28] CCDC 188147 (**11**·PF₆) and CCDC 188995 (**12**·PF₆) contain the supplementary crystallographic data for this paper. These data can be obtained free of charge via www.ccdc.cam.ac.uk/conts/retrieving.html (or from the Cambridge Crystallographic Data Centre, 12 Union Road, Cambridge CB21EZ, UK; fax: (+44) 1223-336-033; or deposit@ccdc.cam.ac.uk). Structure factors are available from the authors via email:xray@caltech.edu.